Astronomy & Astrophysics manuscript no. imf_main
March 12, 2018

SimCADO - The Instrument Data Simulator for MICADO at the ELT

II. Limits to studies of the IMF with the ELT

K. Leschinski[1] and J. Alves[1]

Department of Astrophysics, University of Vienna, Vienna, Austria
e-mail: kieran.leschinski@univie.ac.at

Received TBD; accepted TBD

ABSTRACT

Context. The MICADO near infrared imager on the Extremely Large Telescope will offer diffraction limited imaging over almost an arcminute field of view. With a sensitivity equivalent to the Hubble Space Telescope, MICADO will open up the densest regions of young stellar clusters which are currently limited by confusion. This will allow us to study aspects such as a cluster's IMF in great detail in the Galaxy's densest environments as well as outside the outside the Milky Way.
Aims. The goal of this study was to determine the extent of the parameter space which MICADO will open up for the field of star formation and for studies on the initial mass function. The main question to which we sought an answer was: What is the lowest mass star that MICADO will be able to observe for a given star density and distance?
Methods. We used SimCADO, the instrument simulator package for MICADO to generate observations of 42 dense stellar regions. The star densities of these regions ranged from 10^2 to 10^5 stars arcsec^{-2}and the clusters were placed at distances from 8 kpc to 5 Mpc from the Earth. The lowest reliably observable mass for each cluster was determined via a PSF photometry and subtraction algorithm.
Results. Our results show that star densities of $>10^3$ stars arcsec^{-2}will be easily resolvable by MICADO. The lowest reliably observable mass for clusters in the LMC will be $\sim 0.1 M_\odot$. While it will miss the brown dwarf mass regime in the LMC, MICADO will open up the cores of all dense young stellar clusters in the Magellanic Clouds which are inaccessible with current instruments. We also show that it will be imperative to have good knowledge of the ELT's PSF as the sharp PSF features due to the ELT's segmented mirror will cause many false signals if not treated carefully.
Conclusions. We have shown that MICADO will have access to star clusters 10x denser than what JWST will be able to access, and over 100x denser than those imaged by Hubble. This will allow access to all the members of the densest star clusters in the Milky Way and in the Magellanic Clouds. While the sensitivity of MICADO will no allow us to study the Brown Dwarf regime outside the Milky Way, it will provide extraordinary coverage of the turn over of the IMF in the M-dwarf mass regime in the LMC and SMC.

1. Introduction

The Initial Mass Function (IMF) and its consequences are found in almost all fields of astronomy and astrophysics. It is the empirically derived mass distribution of stars produced during a star formation event. In galactic astronomy the IMF is important because it determines not only the fate of the environment surrounding a star formation region, but in the longer term also the composition of older stellar populations as well as the galaxy as a whole. The relative numbers of low to high mass stars also has a huge impact on the mass cycle of a galaxy. The more mass is locked up in low mass stars, the less smaller the reservoir of gas for the next generation of stars is. For archeoastonomy, the IMF is a critical parameter for determining the star formation history of a galaxy. On the more theoretical side, hydrodynamic simulations of galaxies and cosmological simulations of galaxy clusters use the IMF to determine the strength of feedback mechanisms governing the movement of energy and material. In short the IMF is an extremely important parameter in astronomy. Some may find it humorous that for all its importance, the shape of the IMF is still determined empirically and its origins are hotly debated.

In his original work, Salpeter (1955) used a single power law distribution with a slope of 2.35 to describe the IMF for masses greater than $\sim 0.5 M_\odot$. This was later modified as a series of broken power laws to include the stars below $0.5 M_\odot$ by Kroupa (2001). In contrast Chabrier (2003) proposed a log-normal distribution with a power law modification for the high and low mass regions. As the two descriptions are very similar in the most "observed" region between $0.1 M_\odot$ and $10 M_\odot$, it has proved very difficult to decide which model more aptly describes the IMF.

Furthermore regardless of where observers look, if appears that the shape of the IMF is a constant. Each star forming region produces on average the same amount of stars per mass bin as any other star forming region. Conclusive deviations from accepted IMF are elusive, yet there is one major aspect stopping general acceptance of a universally constant IMF: the fact that we can only observe the lower mass end of the IMF in our own galaxy. Table 1 shows, even in the closest star forming galaxies like the Large and Small Magellanic Clouds, only the Hubble Space Telescope (HST) has the sensitivity to reach the lower mass stars (See references in Table 1). Long exposures with HST can reach just below the first break in the Kroupa power law at $\sim 0.5\, M_\odot$ (Da Rio et al. 2009; Kalirai et al. 2013; Geha et al. 2013), but not far enough into the lower mass regions to put constraints on the shape of the IMF in extragalactic environments. Adding to observers' woes is the lack of spatial resolution. At the distance of the LMC, star forming regions can contain anywhere from 10^2 to 10^5 stars arcsec^{-2}. A perfect example of why current studies struggle to reliably determine the IMF for dense stellar populations outside of the Milky Way is given in Figure 1 of Sirianni et al. (2000). The picture shows a cluster core being completely dominated by the flux of the brightest stars. Thus studies of the IMF are limited to the outer regions of these clus-

Table 1. Mass limits for studies of the IMF outside the Milky Way with the Hubble Space Telescope. It should be noted that for the study by Gallart 1999 the global star formation history was consistent with a Salpeter slope, rather than a Salpeter slope being extracted from the photometric data.

Galaxy	Target	Distance kpc	Mass range $M_\odot$	IMF Slope(s)	Break Mass $M_\odot$	Reference
LMC	R136	50	2.8-15	2.22		Hunter 1995
LMC	NGC 1818	50	0.85-9	2.23		Hunter 1997
LMC	R136	50	1.35-6.5	2.28, 1.27	2.1	Sirianni 2000
LMC	LH 95	50	0.43-20	2.05, 1.05	1.1	Da Rio 2009
SMC	NGC 330	62	1-7	2.3		Sirianni 2002
SMC	NGC 602	62	1-45	2.2		Schmalzl 2008
SMC		62	0.37–0.93	1.9		Kalirai 2013
Hercules		135	0.52-0.78	1.2		Geha 2013
Leo IV		156	0.54-0.77	1.3		Geha 2013
Leo I*		250	0.6-30	2.3		Gallart 1999

ters where star densities are low enough for individual stars to be resolved. The age of a cluster and the resulting level of mass segregation can also skew the results when considering the IMF in large clusters (Lim et al. 2013), however without being able to study the core of such clusters outside the Milky Way, it is difficult to determine to what extent this plays a role. Thus in order to study the lower, and arguably most interesting, part of the IMF in nearby galaxies we will need telescopes with higher spatial resolution and better sensitivity than the current generation of ground and space based telescope.

In the middle of the next decade, the generation of the extremely large telescopes will begin. ESO's Extremely Large Telescope (ELT) (Gilmozzi & Spyromilio 2007) with the help of advanced adaptive optics (Diolaiti 2010) will offer spatial resolution at the diffraction limit of a 40m-class mirror. This will provide an improvement of a factor of ~15 over HST and a factor of ~6 over the future JWST telescope. Combined with the ~978 m^2 collecting area, the ELT will have at least the same sensitivity as the HST in sparse field and will be able to observe much deeper in crowded fields. The MICADO instrument (Davies et al. 2010, 2016) will be the ELT's first-light near-infrared (NIR) wide-field imager and long slit spectrograph. With a plate scale of 4 mas and an AO corrected field of view of almost a square arcminute, MICADO aims to address exactly this niché.

Determining to what extent MICADO will improve our ability to study the IMF and other properties of dense stellar populations is the main focus of this paper. In this paper we have attempted to addressed the following two questions: What is the lowest mass star that MICADO will be able to observe for a given density and distance? What instrumental effects will play a critical role when undertaking such studies with MICADO and the ELT? In our quest for answers to these questions we used SimCADO, the instrument data simulator for MICADO (Leschinski et al. 2016), to simulate a wide range of densely populated clusters at various distances. The current version of SimCADO takes into account all the major and most of the minor spatial and spectral effects along the line of sight between the source and the detector. We used the software to generate realistic images of our model clusters and then conducted several iterations of PSF photometry and star subtraction to extract as many stars as possible from the simulated observations. The extracted stars were compared with the input catalogue to determine the completeness of the extraction and to define a "limiting reliably observable mass" for the different cluster densities and distances.

This paper is organised in the following way: Section 2 describes the clusters used in our simulations and how the simulations were run. In this section we also describe the algorithm for detecting and subtracting stars in the simulated images. In Section 3 we describe the results of the simulations and discuss their validity in the context of possible future observations of real young stellar clusters. Section 4 summarised our results.

2. Data sets

The best way to determine the IMF is to look at a population of stars which is still young enough that all the original members are still around, yet old enough that the main phase of star formation activity is over. If the population is too young, it won't have finished forming all it's stars. Too old and the most massive members will already have gone supernova. Dynamical effects will also mean that several members have "~~run away~~" from the cluster. Ideally the population should also be old enough for any remaining gas and dust to have be expelled of dispersed. Unfortunately such ideal conditions don't exist. Star formation happens over a period of several million years. The most massive stars chew through their hydrogen reserves within the first several ten million years and moves off the main sequence. Given that the dispersion time for newly formed stellar clusters is on the order of hundreds of millions of years, at any point in time relatively few of the observable new clusters will be so youthful. The majority of IMF studies focus on the clusters which come closest to meeting these conditions - namely open clusters (OC) and young massive clusters (YMC). It should be mentioned that OB Associations also provide a laboratory for studying the IMF. However as these are older and more spread out, the chances of contamination from background sources and missing ejected stars is higher. Furthermore, the high mass end of the IMF cannot be observed as the highest mass stars have already left the main sequence, and some have ended as supernova.

2.1. Parameter Space

The HST has a diffraction limit of ~0.1" at 1.2 μm and can reach magnitudes of up to J=28.6^m (Rajan & et al. 2011) in a 10 hour observation. Using AO assisted ground based instruments such NACO at the VLT, diffraction limited observations can be achieved over small (~1') fields of view. The diffraction limit of the VLT telescopes is ~0.03" at 1.2 μm , however NACO only has a sensitivity limit of around J=24^m . Given the As boundary conditions for our suite of artificial clusters we took the resolution limit of HST. Assuming on average one star per FWHM, this gave us a lower density of 100 stars arcsec^{-2}. To set an upper boundary we first took the theoretical diffraction

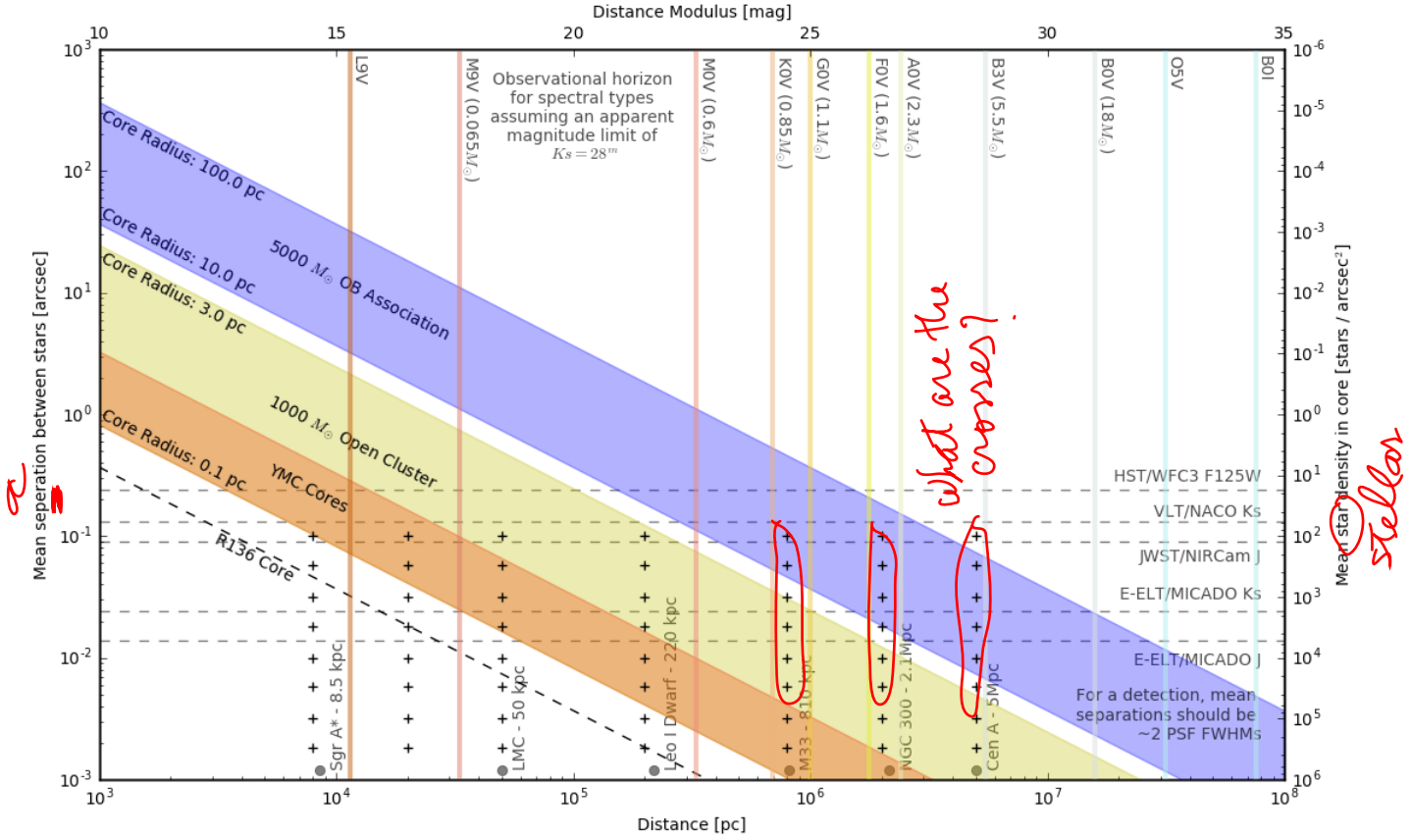

Fig. 1. The parameter space covered by the simulated clusters in this study (crosses) compared to the estimated core star densities for the three major categories of young stellar populations: open clusters (green), young massive clusters (orange), and OB associations (blue). The vertical lines represent the furthest distance at which a certain type of main sequence star will still be above the detection limit of MICADO, i.e. Ks=28^m . The dashed horizontal lines show the theoretical confusion limit for MICADO, JST, HST and NACO/VLT. The confusion limit assumed an average minimum distance of 2x the PSF FWHM between all stars above Ks=28^m . Obviously for NACO confusion ~~would~~'t play as much of a role as the instruments sensitivity limit is Ks~24^m .

limit of the ELT: 7 mas at 1.2 μm , or 2x10^4 stars arcsec^{-2}. As distance increases the sensitivity of an instrument reduces the effective observed star density, as the faintest stars are no longer detectable as individual objects. To avoid any possibly misleading results because of this we increased the upper star density limit to 5x10^5 stars arcsec^{-2}.

Current telescopes are capable of detecting almost all main sequence stars above the hydrogen burning limit (~0.8M$_\odot$) within a few kiloparsecs of the Sun. Detecting all main sequence stars in clusters which are further a field, e.g. in the galactic centre at beyond, is where MICADO's increased sensitivity will bring the greatest breakthroughs. Indeed the question of whether the IMF is indeed universal dictates that we study the IMF outside the Milky Way. Therefore we placed our model clusters at distances corresponding to some of the more well known celestial landmarks: The Galactic Centre (~8 kpc), the LMC (~50 kpc), Leo I dwarf galaxy (~200 kpc), M33 ((~800 kpc))[1], NGC 300 (~2 Mpc), and Cen A (~5 Mpc). Figure 1 shows the parameter space covered by average (~1000M$_\odot$) open clusters with radii between 0.1 pc and 3 pc and average OB Associations (~5000M$_\odot$) with radii between 10 pc and 100 pc as distance from Earth increases. The lower bounds of the open cluster parameter space also covers the cores of YMCs. Average cluster properties were derived for the OB Associations from Mel'Nik & Efremov (1995), for the open clusters from Piskunov et al. (2007), and for the YMCs from Portegies Zwart et al. (2010).

2.2. Artificial clusters

The artificial clusters created for this study are shown as crosses in Figure 1. The size of each cluster was set at 2"x2" (See section 2.3). The cluster was populated by continually drawing stars from an IMF until the required area density was reached. The mass of each star was drawn at random from an IMF distribution with minimum and maximum masses of 0.01M$_\odot$ and 300M$_\odot$. The IMF followed a standard Kroupa (2001) broken power law distribution with breaks at 0.08M$_\odot$ and 0.5M$_\odot$ and standard slope exponents[2]. The absolute J and Ks magnitudes for each star were calculated by interpolating Table 5 in Pecaut & Mamajek (2013)[3] for the given mass. The requisite distance modulus for the cluster was added to give each star an apparent magnitude. The stars were assigned random coordinates within the observa-

[1] The authors recognise that the location of the ELT in the southern hemisphere means that M33 will effectively be unobservable. We provide this data point because M33 will, with luck, be visible to the Thirty Meter Telescope.

[2] By "standard" we mean: α=0.3 for (0.01, 0.08)M$_\odot$, α=1.3 for (0.08, 0.5)M$_\odot$, and α=2.3 for (0.5, 300)M$_\odot$ as defined in Kroupa (2001)

[3] Masses are actually not given in Table 5, but rather in the online suppliment at `http://www.pas.rochester.edu/~emamajek/EEM_dwarf_UBVIJHK_colors_Teff.txt`

tional bounding box. Although true clusters follow some sort of luminosity profile, and hence density profile, for this study we were primarily interested in the densest regions, i.e. the worst case scenario. Hence we made our core regions homogeneously dense. In real observations the decline in density with radial distance will therefore be advantageous and offer an improvement over our pessimistic approach.

2.3. Observations

To "observe" our clusters we used the standard imaging mode of SimCADO (Leschinski et al. 2016) which mimicked observations with the wide-field mode of MICADO at the ELT. The core regions of open clusters and YMC are on the order of ~1-5 pc wide (Portegies Zwart et al. 2010). At a distance of 200 kpc (~Leo 1 Dwarf), this translates to an angular size of 1-5". Thus we thought it safe to assume that the star density within the inner 2"x2" region should remain relatively constant. For the sake of computational effort we decided to restrict to observations to this 2"x2" window in the centre of the detector.

At the very least multi-band photometry is required to determine the mass of a star. Therefore detections in at least the J and Ks filters is necessary. We deemed a detection in the Ks filter to be critical for any study of the IMF and therefore restricted our observations to the the Ks filter. The reason for this is as follows: The FWHM of the 2.2μm PSF is significantly wider than for the 1.2μm PSF. If a source is undetectable in the Ks filter it will not be detectable in the J filter. Given the AO-nature of the observations and the expected reduced Strehl ratio at 1.2μm (Clénet et al. 2016), it could be argued that detections in the J filter will be more difficult. In the end the PSF FWHM is a fundamental limit of physics, whereas the Strehl ratio is a question of engineering and optical design. Hence we deemed a detection in the Ks filter to be the critical point for determining the mass of cluster members. This assumption comes with it's own set of problems which will be discussed in a later paper.

Exposure times were kept to 1 hour for no other reason than observing time at the ELT will be in very high demand once it comes on line and observations in two or more filters are needed to accurately determine the cluster mass function.

2.4. Source extraction and matching

Figures .1 and .2 in the Appendix show a graphical representation of the process described in this section. They show two examples of "observed" clusters placed at a distance of 50 kpc and containing 10^3 and 10^4 stars arcsec^{-2}respectively. The stark features of the SCAO PSF[4] are clearly visible in the image. The diffraction core of the PSF is however still well modelled by a Gaussian distribution. To find and measure the stars in the images we used the following method:

1. Use the `DAOStarFinder` class from `photutils` (Bradley et al. 2017) to find the brightest star in the image
2. Find the centre the star in a 5x5 pixel window around the coordinates given by `DAOStarFinder`
3. Fit a 2D Gaussian profile to the core of the star
4. Scale an image of a reference star to match the amplitude, baseline and offset of the found star
5. Subtract the scaled reference star from the image
6. Repeat until `DAOStarFinder` no longer finds any sources above 5σ

In practice we found that we could subtract ~100 stars at once and thus greatly increase the speed of the process. The amplitudes and baselines were converted to magnitudes based on the reference star. Our reference star was a solitary "field" star with a magnitude of Ks=15, observed for the minimum MICADO exposure time of 2.6 s. We calculated masses for each star based on the observed fluxes in the Ks filter. This step is only permissible because of the simplified context of this study. We are free to equate the luminosity function with an equivalent mass function because all our test clusters have the intrinsic property that they only contain main sequence stars and the luminosity and mass functions enjoy a one-to-one relationship in the Ks filter, mathematically speaking. Furthermore, our primary goal is to determine what the lowest possible observable mass is, based on how well MICADO will perform in crowded field - not to directly measure the mass of the original stars. We feel that this step does not detract from achieving the goal of this study.

Finally we cross-matched the coordinates of the extracted sources with the original table of coordinates to determine what fraction of stars were correctly detected with our algorithm. Due to noise an confusion from very close stars the centroid coordinates of the extracted star was not always exactly equal to the original coordinates. The cross-matching algorithm was instructed to search for the closest star within a 25 mas radius. If a fainter or brighter star happened to be closer, then the algorithm chose this star from the catalogue as the match. We determined whether the extracted masses for stars in a certain mass bin were "reliable" by binning the extracted stars according to mass. We then took the mean and standard deviation of all stars within a mass bin. As long as the mean extracted mass to true mass ratio was in the range 1.0±0.1 and the standard deviation was less than 0.1, the mass bin was classed as reliable. By this definition the lowest reliably detectable mass for a cluster was given by the lower edge of the lowest mass bin which satisfied these criteria.

3. Results and Discussion

3.1. Lower observable masses for given star densities

The first of the questions we asked with this study - "What is the lowest mass star that MICADO will be able to observe for a given density and distance?" - can be answered by Figure 2. For each of the distances and densities we have plotted the lowest reliable mass bin. The scatter in the plot reflects the random nature of the simulations. The positions of the stars in each of the test cluster were randomised, the sampling of the mass function was random and shot noise was applied to the image as part of SimCADO's read-out process. Thus no two clusters were the same. Additionally the accuracy of the limiting observable masses is limited by small number statistics. Due to time constraints each cluster configuration was only run once. We therefore only have one data point for each density and distance. The bin size used for the reliability statistics was set to 0.2 dex, and is therefore the uncertainty in the limiting observable mass.

From Figure 2 we can immediately see the two limiting regimes of sensitivity and crowding. The flat regions in Figure 2 show the densities for which MICADO will be sensitivity limited and the diagonal regions show when crowding is the limiting factor. For example observations of a cluster at a distance of 8 kpc observations will always be crowding limited. At a distance of

[4] The PSF user here was from a simulation of the SCAO mode from MAORY. It was only released internally within the MAORY consortium. By default the SimCADO package comes with a SCAO PSF generated by the MICADO consortium, which is in the public domain.

Figure: Images of artificial clusters?

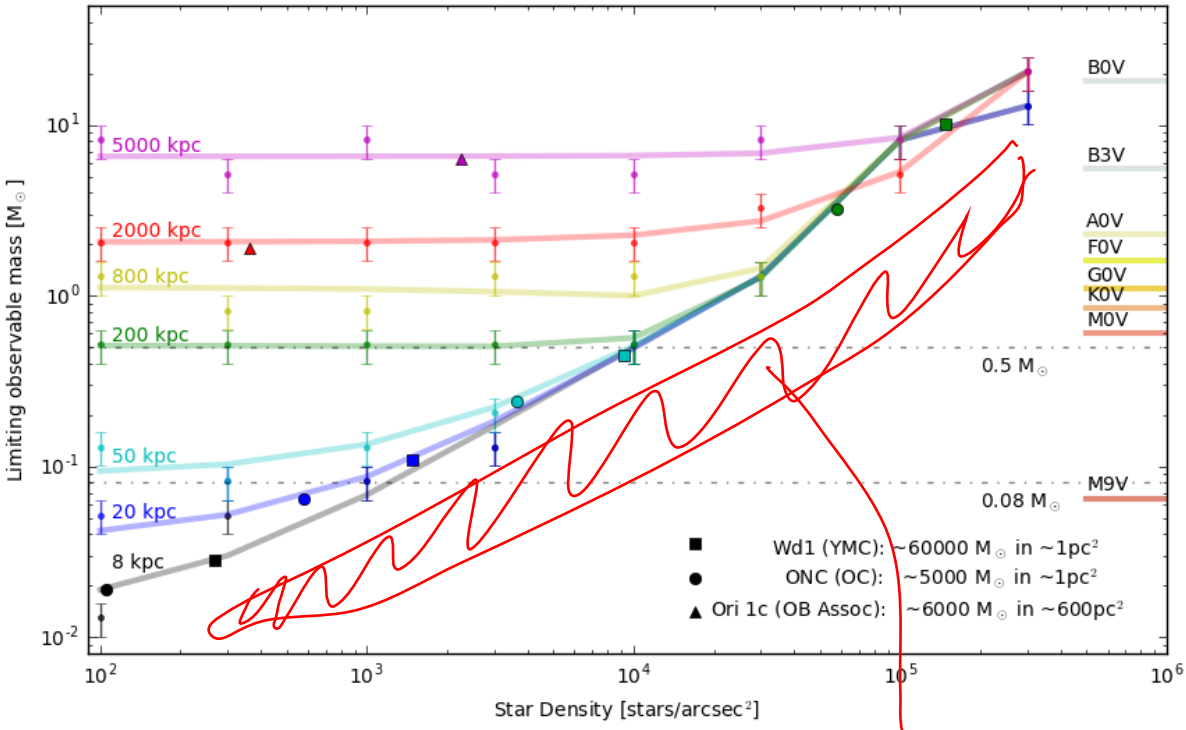

Fig. 2. The main result of this paper. How far down the IMF can we go for a given density and distance.

200 kpc observations will limited by sensitivity up to a density of 10^4 stars arcsec^{-2}, thereafter crowding will be the dominant factor. At 5 Mpc all observations will be sensitivity limited. So the sake of reference we have also included in Figure 2 the approximate star densities for three well known young clusters *if they were located at the distance of the test cluster*. For example, if the YMC Westerlund 1 were to be located in the LMC, it would fall in to the crowding-limited regime for MICADO. The lowest reliably observable mass in the densest region of the core would still be ~0.5 $M_\odot$. This is equivalent to what HST would be capable of for only the outer most regions of the cluster. For clusters in the LMC with star densities less than 10^3 we see that MICADO will be limited by sensitivity to masses above 0.1 $M_\odot$. While this mass is only 0.3 $M_\odot$ lower than what current observations with Hubble can achieve, it should be emphasised that this jump of "only" 0.3 $M_\odot$ will reveal the majority of M-type stars, which account for almost three quarters of all main sequence stars (**?**). Given that limit of current studies is around the 0.5 $M_\odot$ knee from Kroupa (2001), opening up this range will allow future studies to pin down exactly what the shape of the IMF looks like in the LMC. It should also be noted the majority of young clusters have core which are less dense than that of Westerlund 1, and therefore the limiting observable mass will also be lower than the 0.5 $M_\odot$ mass quoted a YMC in the LMC. Given MICADO's resolving power it will therefore also be possible to determine to what extent mass segregation has played a role in previous studies of the IMF in the LMC. More to the point MICADO will enable us to understand the apparent deviations from the Salpeter IMF as reported by **dario, geha, kalaraii**.

At distances of 100 kpc to 200 kpc and with careful photometry and longer observations MICADO should be able to detect stars down to the sensitivity limit of 0.5 $M_\odot$. This will only be possible though for clusters with star densities less than 10^4 stars arcsec^{-2}. As a reference an ONC-like cluster at a distance of 200 kpc will have a star density on the order of 10^5 stars arcsec^{-2}. Such observations will be useful for determining the composition of OB associations and sparser (older) open clusters, if there were any present in the non-magellanic satellites of the Milky Way. Nevertheless MICADO will still allow us observe the fabled 0.5 $M_\odot$ knee in the field population of the nearest low metallicity dwarf spheroidal galaxies.

Closer to home MICADO should be able detect the 10 M_J objects in an ONC-like clusters at a distance of 8 kpc. The Arches cluster is obvious candidate for such studies, and given its proximity to the galactic centre makes it an ideal case to study the the IMF under extreme conditions. The main hindrance to such observations is not the almost 2 mag of variable Ks-band extinction along the line of site (Espinoza et al. 2009), but rather the brightest stars in the cluster. The effectiveness of MICADO observations will also be limited by the brightest stars in the field. Leschinski (2018, submitted) state that point sources with magnitudes Ks>14.8^m will saturate the MICADO detectors within the 2.6 s minimum exposure time. There are very few regions in the cores of Milky Way open clusters which don't contain stars brighter than Ks~15^m , making possible MICADO observations of these regions difficult.

3.2. The cores densities of young star clusters

The second of the questions we asked with this study was "What instrumental effects will play a critical role when undertaking such studies with MICADO and the ELT?". The instrumental effect which would play the largest role regarding the accuracy of the estimates given here is our knowledge of the PSF. For this

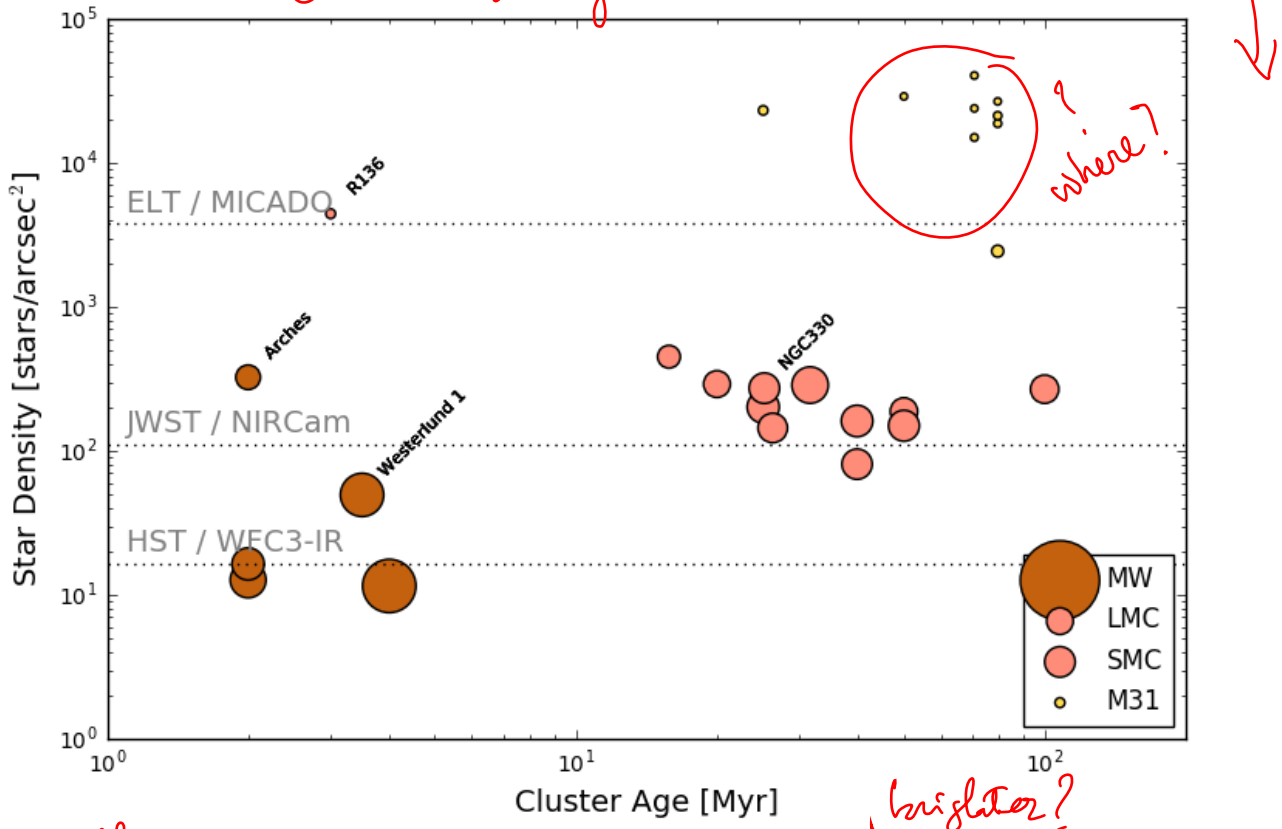

Fig. 3. The star densities in the cores of the clusters listed in Table .1 assuming a sensitivity limit of Ks=28^{m} . The densities shown here take into account the sensitivity limit and therefore are only for the potentially observable stars, i.e. any low luminosity stars with Ks>28^{m} are omitted from the density calculation. This is equivalent to all stars in the Milky Way, M-class stars and bright in the LMC, and G-class stars and bright in M31. Only clusters from Portegies Zwart et al. (2010) which had a defined core radius, r_c, are shown here. The size of the circles is proportional to the relative on-sky size of the cluster cores. The colours reflect the lowest possible reliably observable mass, as shown in Figure 2 and listed in Table .1. The dashed lines in this figure represent the optimal resolving capability of the HST, JWST and ELT. We define optimal density as the mean distance between stars is equal to 2.5x the PSF FWHM. Given the predicted PSF shapes for the latter two telescopes, these lines may prove to be somewhat optimistic. Nevertheless the graphic illustrates the point that the youngest YMCs are far too dense for either HST or JWST observations. Thus it will require the ELT (or similar) to study the most heavily populated regions of these clusters.

study we used a single SCAO PSF. We assumed that the PSF orientation stayed the same for the length of the observation. Consequently we had a very good model of our reference star for the PSF subtraction. This will obviously not be the case for real observations as the pupil of the telescope will rotate with respect to the sky, causing an axial broadening of the PSF over the course of an observing run. On the one hand this broadening should improve the results from our subtraction method as it will smooth out many of the sharp features of the instantaneous PSF. On the other hand we will lose information on both the structure of the PSF and the extent of the wings. Thus the PSF subtraction algorithm will less accurately be able to estimate the background level when fitting the reference PSF to a star. As a consequence faint stars caught in the PSF wings of the brighter stars may not be detected as often as they would be if the PSF remained rotationally aligned with the sky. A hybrid approach to the faint star subtraction problem may be the following: Subtract the brightest stars from each individual exposure using an instantaneous PSF derived from the brightest stars in that exposure, then stack the residual images and extract the faintest stars using a rotationally broadened PSF. Further investigation is required to determine whether this approach would indeed increase the detection rate for faint stars.

Although it may seem obvious, one final point is worth mentioning. From our simulations it is clear that resolving star densities of 10^3 stars arcsec^{-2}is well within the capabilities of MICADO. With an optimised PSF fitting and subtraction algorithm, extracting upwards of $5x10^3$ stars arcsec^{-2}should also be in the realms of possibility. $5x10^3$ stars arcsec^{-2}is equivalent to approximately one star in the equivalent area of ~2.5 H-band PSF FWHMs. This is similar to being able to resolve every star in the core of an ONC-like cluster in the LMC. For JWST and HST the equivalent star densities are 160 stars arcsec^{-2}and 20 stars arcsec^{-2}respectively. Although MICADO may not have the sensitivity of a space-based telescope, the resolving power will give us full access to the core populations of dense stellar clusters in the major satellites of the Milky Way.

3.3. The cores densities of young star clusters

The simulations are a nice theoretical exercise, however without an application to observations they are not all that useful. Figure

3 shows the estimated star densities in the cores of the open clusters and YMCs compiled by Portegies Zwart et al. (2010). The density values, $\log_{10}(\rho)$, only take into account the stars with apparent magnitudes above the sensitivity limit of MICADO and thus reflect the "real" observable density for the clusters (Also listed in Table .1). The limits set for HST, JWST and MICADO are the critical star density above which our extraction algorithm struggles to detect and remove more than 90% of the stars in a field. We find that for the Galactic clusters, the resolution of JWST will be sufficient to resolve all stars in the cluster's core down to the sensitivity limit of the instrument. We will however definitely need the resolution of MICADO to resolve the cores of the young clusters in the Magellanic clouds. Based on the compiled ages listed in Portegies Zwart et al. (2010) MICADO will give us access to the cores of young clusters in the LMC which cover a wide range of ages. This allow a much deeper understanding of the dynamical processes (e.g. evaporation, core collapse, etc.) involved in the evolution of these clusters. Additionally observations of a "time" series of LMC clusters will give a much better picture of how the initial mass function evolves into the present day mass function, and how the dynamical evolution of the cluster influences the observations and determination of a cluster's IMF.

4. Conclusion

MICADO and the ELT will offer us the chance to finally resolve the core populations of star clusters outside the Milky Way. By turning MICADO towards young stellar clusters we hope to finally answer the question as to whether the IMF is indeed universal, or whether the shape of the distribution changes when we leave the Galaxy. Currently the answers are locked up inside young stellar clusters, which by nature have very high star densities. Observations of these clusters are primarily limited by confusion. Exactly how much of the stellar populations will be visible to MICADO is what we wanted to address with this study.

This study aimed to answer two questions: What is the lowest mass star that MICADO will be able to observe for a given star density and distance? And what instrumental effects will play a critical role when undertaking such studies with MICADO and the ELT? In order to answer these we used the instrument simulator for MICADO (SimCADO) to generate "observations" of 42 dense stellar regions. These regions had star densities similar to what would be observed if one were to place an open cluster or a young massive cluster at various distances from Earth. Here we present a brief summary of the results:

- We have shown that MICADO will easily be able to resolve stellar populations with star densities of 10^3 stars arcsec^{-2}. With proper knowledge of the PSF and an optimised detection and subtraction algorithm densities of 5000 stars arcsec^{-2}should also be achievable.
- Given that MICADO observations will be bound by the instrument's sensitivity to both the brightest and faintest sources in the field of view, MICADO is best suited to investigate the shape of the IMF in clusters in the outer edges of the Milky Way as well as the nearest galaxies. For real world science cases this means that the cores of dense young star clusters such R136 in the LMC and NGC330 in the SMC will be resolvable with MICADO.
- Observations focussing on the initial mass function of clusters in the LMC we will be limited by sensitivity, not crowding, to 0.1 $M_\odot$. This means that investigations of the Brown Dwarf knee (~0.08 $M_\odot$) will not be possible outside the Milky Way, however MICADO's resolution will allow the low mass function (0.1 $M_\odot$ <M <0.5 $M_\odot$) to be extensively investigated and well characterised.
- The brown dwarf population will be accessible in the cores of the densest Milky Way clusters, e.g. in the Arches and Westerlund clusters. Objects with masses on the order of 10 M_J will be accessible by MICADO for clusters within 8 kpc of Earth. The only caveat is that an appropriate observation strategy be found to mask the many bright ($m_K s$<15^m) stars in these clusters.
- Finally accurate knowledge of the ELT's PSF will be absolutely essential for good photometry and PSF subtraction algorithms. The sharp structures created by the segmented mirror design lead to many fake low luminosity star detections if either the PSF is not well known or the extraction algorithm isn't capable of differentiating between a star and an artefact of the PSF.

Acknowledgements. SimCADO incorporates Bernhard Rauscher's HxRG Noise Generator package for python (Rauscher 2015). This research made use of POPPY, an open-source optical propagation Python package originally developed for the James Webb Space Telescope project (Perrin et al. 2015). This research made use of Astropy, a community-developed core Python package for astronomy (Astropy Collaboration et al. 2013; The Astropy Collaboration et al. 2018). This research made use of Photutils (Bradley et al. 2017). This research has made use of "Aladin sky atlas" developed at CDS, Strasbourg Observatory, France (Bonnarel et al. 2000; Boch & Fernique 2014). SimCADO makes use of atmospheric transmission and emission curves generated by ESO's SkyCalc service, which was developed at the University of Innsbruck as part of an Austrian in-kind contribution to ESO. This research is partially funded by the project IS538003 of the Hochschulraumstrukturmittel (HRSM) provided by the Austrian Government and administered by the University of Vienna. KL would also like to express his gratitude to Eline Tolstoy for the insightful and helpful comments and discussions regarding future possible observations the ELT.

References

Astropy Collaboration, Robitaille, T. P., Tollerud, E. J., et al. 2013, A&A, 558, A33
Boch, T. & Fernique, P. 2014, in Astronomical Society of the Pacific Conference Series, Vol. 485, Astronomical Data Analysis Software and Systems XXIII, ed. N. Manset & P. Forshay, 277
Bonnarel, F., Fernique, P., Bienaymé, O., et al. 2000, A&AS, 143, 33
Bradley, L., Sipocz, B., Robitaille, T., et al. 2017, astropy/photutils: v0.4
Chabrier, G. 2003, PASP, 115, 763
Clénet, Y., Buey, T., Rousset, G., et al. 2016, in Proc. SPIE, Vol. 9909, Society of Photo-Optical Instrumentation Engineers (SPIE) Conference Series, 99090A
Da Rio, N., Gouliermis, D. A., & Henning, T. 2009, ApJ, 696, 528
Davies, R., Ageorges, N., Barl, L., et al. 2010, in Proc. SPIE, Vol. 7735, Ground-based and Airborne Instrumentation for Astronomy III, 77352A
Davies, R., Schubert, J., Hartl, M., et al. 2016, in Proc. SPIE, Vol. 9908, Society of Photo-Optical Instrumentation Engineers (SPIE) Conference Series, 99081Z
Diolaiti, E. 2010, The Messenger, 140, 28
Espinoza, P., Selman, F. J., & Melnick, J. 2009, A&A, 501, 563
Geha, M., Brown, T. M., Tumlinson, J., et al. 2013, ApJ, 771, 29
Gilmozzi, R. & Spyromilio, J. 2007, The Messenger, 127
Kalirai, J. S., Anderson, J., Dotter, A., et al. 2013, ApJ, 763, 110
Kroupa, P. 2001, MNRAS, 322, 231
Ledrew, G. 2001, JRASC, 95, 32
Leschinski, K., Czoske, O., Köhler, R., et al. 2016, in Proc. SPIE, Vol. 9911, Society of Photo-Optical Instrumentation Engineers (SPIE) Conference Series, 991124
Lim, B., Chun, M.-Y., Sung, H., et al. 2013, AJ, 145, 46
Mel'Nik, A. M. & Efremov, Y. N. 1995, Astronomy Letters, 21, 10
Pecaut, M. J. & Mamajek, E. E. 2013, ApJS, 208, 9
Perrin, M. D., Long, J., Sivaramakrishnan, A., et al. 2015, WebbPSF: James Webb Space Telescope PSF Simulation Tool, Astrophysics Source Code Library
Piskunov, A. E., Schilbach, E., Kharchenko, N. V., Röser, S., & Scholz, R.-D. 2007, A&A, 468, 151
Portegies Zwart, S. F., McMillan, S. L. W., & Gieles, M. 2010, ARA&A, 48, 431
Rajan, A. & et al. 2011, WFC3 Data Handbook v. 2.1 (STSci)
Rauscher, B. J. 2015, PASP, 127, 1144
Salpeter, E. E. 1955, ApJ, 121, 161
Sirianni, M., Nota, A., Leitherer, C., De Marchi, G., & Clampin, M. 2000, ApJ, 533, 203
The Astropy Collaboration, Price-Whelan, A. M., Sipőcz, B. M., et al. 2018, ArXiv e-prints [arXiv:1801.02634]

Table .1 lists

Figures .1 and .2 show the results for two of the 42 simulated observations. Both figures show the case of a cluster located at the distance of the LMC. In each figure the observation of the cluster can be seen along side the residuals of the subtraction process. For clusters with densities lower than 10^3 stars arcsec^{-2}the subtraction process worked very well, with almost all stars being accurately removed (see Fig .1). After this level the effectiveness of the PSF subtraction continually degraded with increasing density. This was to be expected. Figure .2 shows the case for a 10^4 stars arcsec^{-2}cluster. Although the majority of stars were removed from the image, the stars which failed the fitting test remain. This was often due to two sufficiently bright stars being too close together and the fitting algorithm was not able to match a symmetrical Gaussian profile to the pair. These failed subtractions had a knock-on effect where the fainter artefacts of the PSF were detected as stars with lower signal to noise ratios, which increased the number of fake source detections.

The bottom right panels Figures .1 and .2 shows the ratio of real mass to detected mass for each of the stars extracted from the simulated images, as well as the standard deviation for the mass ratio bins. It can be seen that the standard deviation is a good indicator for extraction reliability.

Table .1. The age and observable star densities for a selection of young massive clusters found both in and outside the Milky Way, as listed in Portegies Zwart et al. (2010). The densities have been calculated to only include stars which are brighter than Ks=28^{m} , as fainter stars will not be detectable by MICADO. The table list the parameters for the clusters shown in Figure 3.

Galaxy	Cluster	Distance kpc	Age Myr	log(Mass) $M_\odot$	Core radius arcsec	$\log_{10}(\rho)$ arcsec{-2}	Limiting mass $M_\odot$
			Cores resolvable by HST				
MW	ONC	0.4	1	3.7	100	-1.6	0.01
MW	Trumpler-14	2.7	2	4	10.7	1.1	0.01
			Cores resolvable by JWST				
MW	NGC3603	3.6	2	4.1	8.6	1.2	0.01
MW	Westerlund-1	5.2	3.5	4.5	15.9	1.7	0.01
MW	Quintuplet	8.5	4	4.0	24	1.1	0.04
LMC	NGC2214	50	39.8	4.0	7.5	1.9	0.1
			Cores resolvable by MICADO				
LMC	NGC1847	50	26.3	4.4	7.1	2.2	0.1
LMC	NGC2157	50	39.8	4.3	8.2	2.2	0.1
LMC	NGC1711	50	50.1	4.2	7.9	2.2	0.1
LMC	NGC1818	50	25.1	4.4	8.5	2.3	0.1
LMC	NGC2164	50	50.1	4.2	6.1	2.3	0.1
SMC	NGC330	63	25.1	4.6	7.7	2.4	0.15
LMC	NGC2136	50	100	4.3	6.6	2.4	0.1
MW	Arches	8.5	2	4.3	4.9	2.5	0.04
LMC	NGC1850	50	31.6	4.9	11	2.5	0.1
LMC	NGC2004	50	20	4.4	5.8	2.5	0.1
LMC	NGC2100	50	15.8	4.4	4.1	2.7	0.1
M31	B257D	780	79.4	4.5	0.8	3.4	0.9
			Only outer regions resolvable by MICADO				
LMC	R136	50	3	4.8	0.41	3.7	0.1
M31	B066	780	70.8	4.3	0.10	4.2	0.9
M31	B040	780	79.4	4.5	0.15	4.3	0.9
M31	B043	780	79.4	4.4	0.19	4.3	0.9
M31	B318	780	70.8	4.4	0.05	4.4	0.9
M31	B448	780	79.4	4.4	0.05	4.4	0.9
M31	Vdb0	780	25.1	4.9	0.37	4.4	0.9
M31	B327	780	50.1	4.4	0.05	4.5	0.9
M31	B015D	780	70.8	4.8	0.06	4.6	0.9

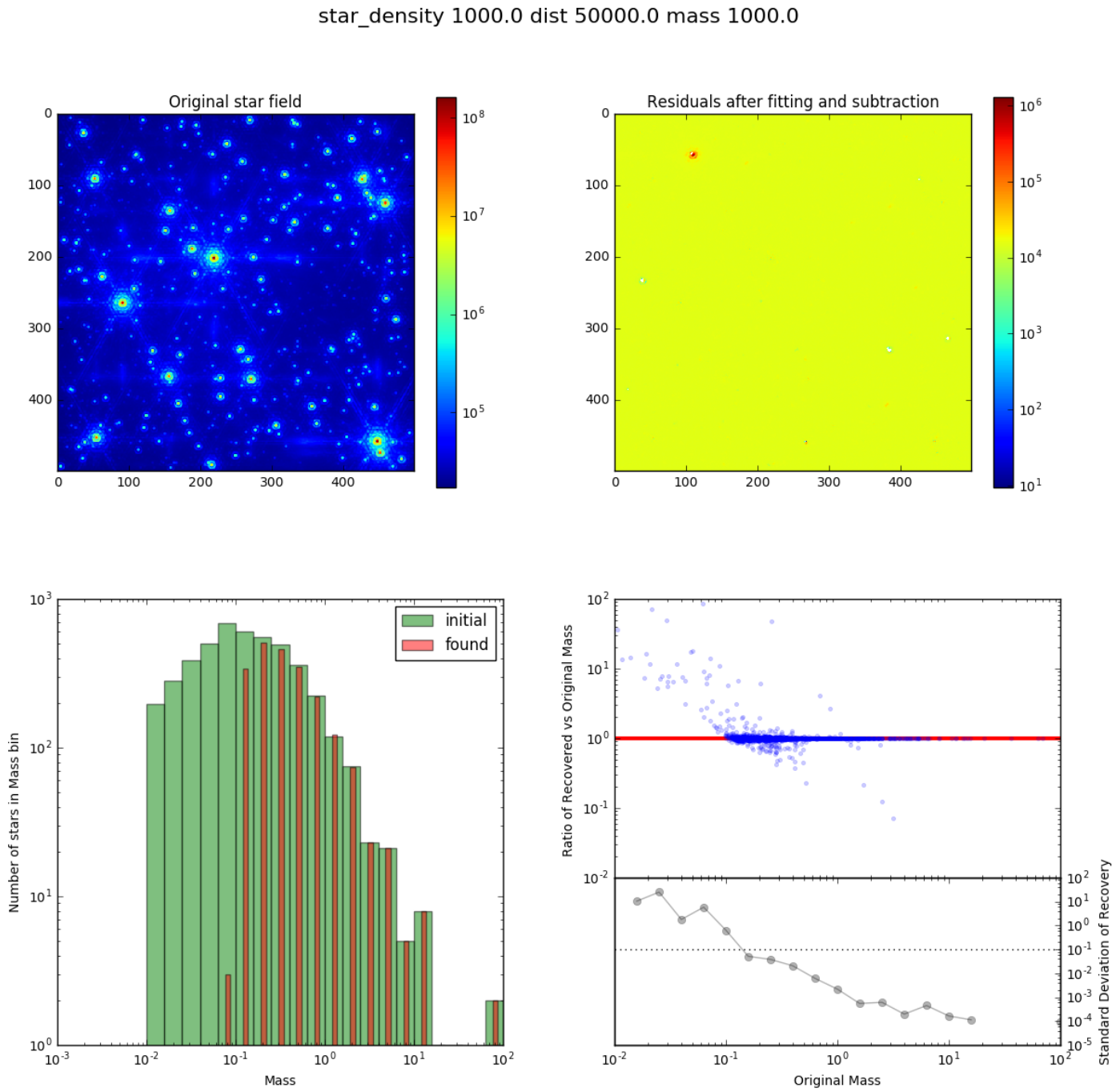

Fig. .1. Results of extracting stars from a 1000 $M_\odot$ cluster

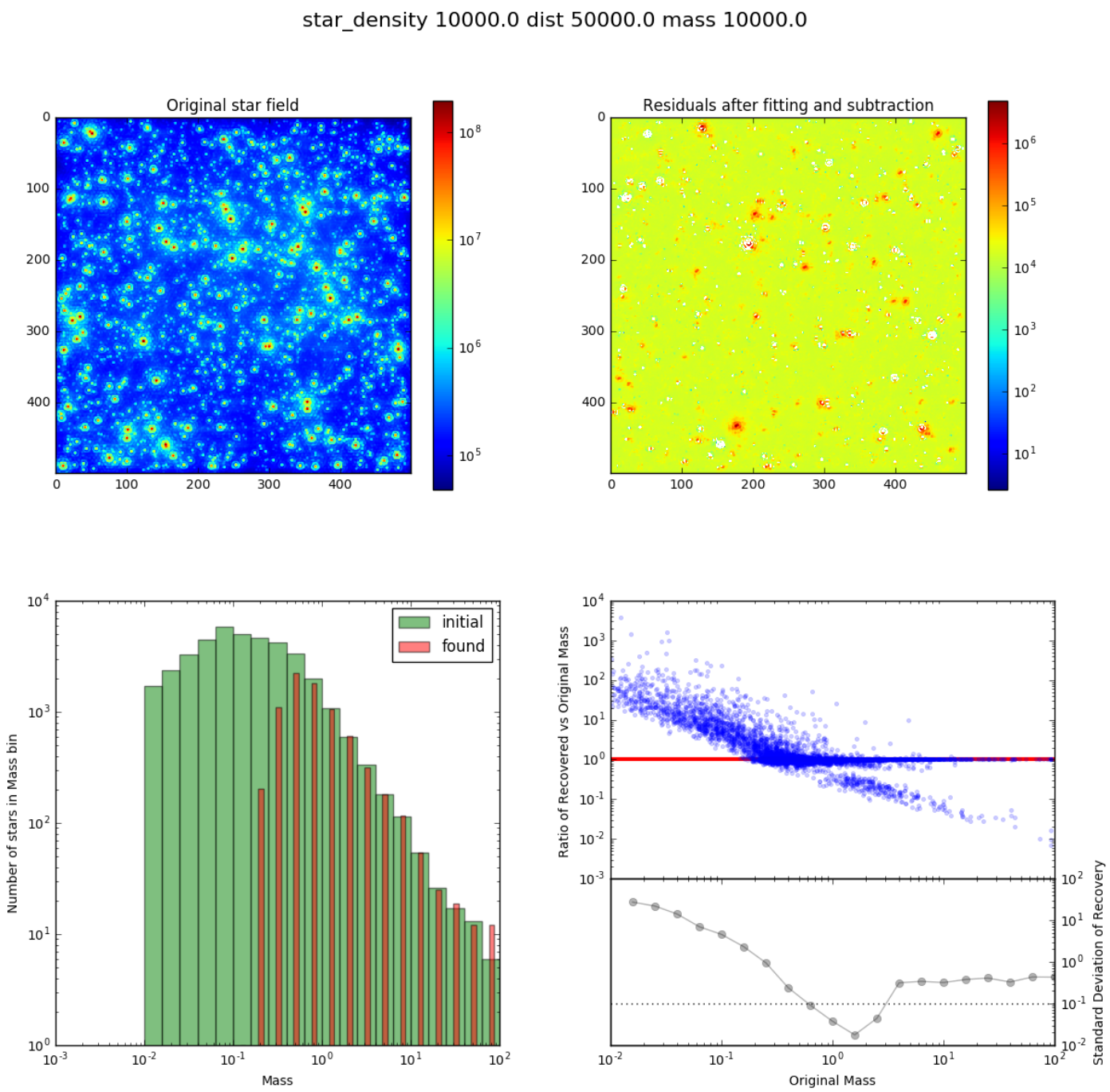

Fig. .2. Same as above but for a 10 000 $M_{\odot}$ cluster